ACS APPLIED MATERIALS & INTERFACES

Research Article

www.acsami.org

Self-Assembly of Conjugated Polymer on Hybrid Nanospheres for Cellular Imaging Applications

Bihua Xia, Xiaoyu Wang, Fang He, Qianling Cui, and Lidong Li*

State Key Laboratory for Advanced Metals and Materials, School of Materials Science and Engineering, University of Science and Technology Beijing, Beijing 100083, P. R. China

Supporting Information

ABSTRACT: A new kind of hybrid core–shell nanosphere was fabricated by combining the in situ formation of Au nanoparticles and covalent cross-linking of biocompatible carboxymethyl starch dialdehyde (CMSD) and chitosan (CTS). When the fluorescent dye poly[9,9′-bis(6″-(*N*,*N*,*N*-trimethylammonium)-hexyl)fluorene-2,7-ylenevinylene-*co*-alt-1,4-phenylene dibromide] (PFV) was assembled on the surface of the hybrid nanospheres through electrostatic attraction, these biocompatible hybrid nanospheres exhibited metal-enhanced fluorescence effects. The fluorescence intensity of (CTS–Au)@CMSD/PFV hybrid nanosphere is 1.43 times that of CTS–CMSD/PFV hybrid nanospheres lacking Au nanoparticle. In addition, the (CTS–Au)@CMSD/PFV hybrid nanospheres exhibit excellent biodegradability upon exposure to enzymatic aqueous solution and good biocompatibility when cocultured with HeLa cervical carcinoma cells; these advantages make them attractive for cellular imaging and biological analysis and detection.

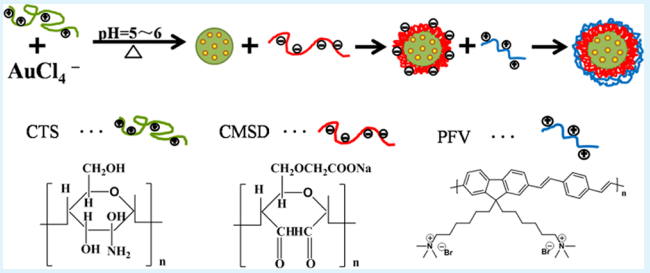

KEYWORDS: *self-assembly, fluorescence, conjugated polymer, hybrid nanosphere, biocompatibility, cellular imaging*

INTRODUCTION

Hybrid nanospheres with different core–shell structures are attracting significant interest because of their unique structure and multifunctional properties, which make them suitable for use in drug release, catalysts, biological assays, and tissues.[1−6] In addition, hybrid nanospheres with core–shell structure that contain functional fluorophores show great potential in biomaterials and biological applications, e.g., fluorescent biomaterials,[7,8] biological sensors and detection,[9−11] and efficient cell imaging and sensing.[12]

Presently, conventional core–shell hybrid nanospheres for live cell imaging applications are typically produced by fabricating functional polymers on the surface of as-prepared metal nanoparticles.[12] However, the synthesis and modification of core–shell hybrid nanoparticles are complicated. The present systems often contain inorganic silica shells or synthetic polymers such as poly(acrylic acid) , polyvinylpyrrolidone, and polymethacrylates, which are derived from fossil resources, to act as interlayers between fluorophores and metallic nanostructures.[13−17] The biocompatibility and biodegradability of these systems are insufficient for in vivo biological studies. To overcome these limitations, we used a highly efficient in situ reduction method and green renewable materials to prepare novel nanospheres. Chitosan (CTS), a polysaccharide with the ability to reduce and chelate metal ions,[18] was selected to form a CTS–metal composite.[19−22] Carboxymethyl starch dialdehyde (CMSD), which is widely used in drug delivery and polyelectrolyte complexes and as a coating agent,[23−27] was chosen as a biocompatible material to form the shells of the hybrid nanospheres. Although these materials possess many advantages including biocompatibility, renewability, and low cost, CTS and CMSD have seldom been applied in core–shell hybrid nanosphere systems.[23,27]

Core–shell hybrid nanospheres with metal cores usually exhibit metal-enhanced fluorescence (MEF), which has attracted much attention because of its wide range of potential applications.[28−30] The strong plasmonic resonance from nanostructured metallic surfaces (such as those of Au nanoparticles) can enhance the fluorescence intensity of fluorophores within a certain distance. To date, many metallic nanostructures with various morphologies have been employed to study MEF.[31,32] MEF depends on interaction distance, so we have used hybrid nanocomposites containing responsive Ag nanoparticles to control MEF.[12,33−35] However, there are few reports investigating the use of natural biocompatible MEF systems for cellular imaging.[36] Introduction of CTS and starch into hybrid nanocomposite systems is highly desirable for cell experiments under biological and physiological conditions.

In this study, we developed novel biocompatible (CTS–Au)@CMSD hybrid nanospheres, which were fabricated by the combination of in situ preparation of Au nanoparticles and covalent cross-linking of CTS and CMSD.[37] In this system, Au nanoparticles incorporated in CTS matrices form the core of the nanospheres, while CMSD forms a shell through

Received: September 10, 2012
Accepted: October 26, 2012
Published: October 26, 2012

electrostatic adsorption and consequent covalent bonding between the amino and aldehyde groups.[27] The fluorophore poly[9,9′-bis(6″-(*N*,*N*,*N*-trimethylammonium)-hexyl)fluorene-2,7-ylenevinylene-co-alt-1,4-phenylene dibromide] (PFV) was adsorbed on CMSD through electrostatic adsorption. The as-prepared nanospheres exhibited bright fluorescence because of strong MEF. The nanospheres were used to image HeLa cervical carcinoma cells, and their cytotoxicity was evaluated using the 3-(4,5-dimethylthiazol-2-yl)-2,5-diphenyltetrazolium bromide (MTT) viability assay.

EXPERIMENTAL SECTION

Materials and Measurements. PFV was synthesized according to our previous publication.[15] Carboxymethyl starch (CMS, pharmaceutical grade), $HAuCl_4{\cdot}4H_2O$, pancreatin (USP grade), and amyloglucosidase (liquefied, 10^5 U/mL, laboratory grade) were purchased from Aladdin Chemistry Co., Ltd. CTS (degree of acetylation of 80−95%, M_w = 250 000 g/mol, PDI = 1.5, monomodal distribution) was purchased from Sinopharm Chemical Reagent Co., Ltd. Sodium periodate and acetic acid (analytical grade) were purchased from Beijing Chemical Reagent Co., Ltd. 1-Ethyl-3-(3-dimethylaminopropyl) carbodiimide (EDCI) was purchased from J&K Scientific, Ltd. All reagents were used without further purification unless stated otherwise. Fourier transform infrared (FTIR) spectra of CMS, CMSD, CTS, and CMSD−CTS composites were measured using KBr pellets with a Nicolet 170SX FT-IR spectrometer. The ^{1}H NMR spectra was recorded on 600 MHz AC Bruker spectrometer. The maximum surface plasmon absorption of Au nanoparticles was measured on a Hitachi U3900 spectrophotometer. Transmission electron microscope (TEM) images were recorded on a JEM 2100 TEM with an accelerating voltage of 120 kV. Environmental scanning electron microscope (ESEM) images were recorded on a Quanta 200FEG scanning electron microscope with an accelerating voltage of 4.0−6.0 kV. The hydrodynamic diameters of the nanospheres were measured by dynamic light scattering (DLS) using a Nano ZS90 zetasizer (Malvern Instruments Ltd.) at room temperature. Fluorescence spectra of samples were obtained on a Hitachi F-7000 luminance spectrometer. Cellular images were taken with an Olympus IX71 fluorescence microscope using a 100 W mercury lamp as the light source. The calcination experiment was measured by Muffle furnace (SX_2-2.5-12) at 700 °C for 2 h.

Preparation of CMSD. CMS and sodium periodate (2:1 molar ratio) were dissolved in water with aqueous solution concentration of 35% (w/w) and vigorous mechanical stirring.[38] The pH of the mixed solution was kept at 7.0, and the reaction temperature was set at 37 °C. After 12 h, the slurry was filtered. The product was washed with deionized water five times and then dried under vacuum at 50 °C for 24 h and then 120 °C for another 24 h to obtain a gray powder of CMSD.

Preparation of CTS−Au Nanocomposites. All glassware was cleaned in a bath of freshly prepared aqua regia (HCl/HNO_3 = 3:1) and then rinsed thoroughly with H_2O prior to use. Prior to the preparation of nanospheres, 0.1% (w/w) CTS solution was prepared by dissolving an amount of CTS in 10% acetic acid. Because of the limited solubility of CTS, the mixture was first stirred and then filtered through a 5 μm Millipore syringe filter to remove any undissolved impurity. Certain concentrations of 100 μL of $HAuCl_4$ solution (0.1 M) was added dropwise to stirred aqueous CTS solution (10 mL). The mixture was heated at 85 °C for 2.5 h in the dark using an oil bath, giving a red CTS−Au nanocomposite solution. The resultant mixture containing CTS−Au nanocomposites was centrifuged and redispersed in acidified distilled water (pH = 5−6) at least three times.

Preparation of (CTS−CMSD)/PFV and (CTS−Au)@CMSD/PFV Nanospheres. A certain amount of CTS solution or the centrifuged CTS−Au nanocomposite solution was added dropwise to an equal volume of aqueous 3% (w/w) CMSD solution. EDCI was added to the mixture as a catalyst, and then, the mixture was stirred for 24 h at room temperature to form pure CTS−CMSD and (CTS−Au)@CMSD nanosphere solutions; the final concentration of EDCI was 1.6×10^{-5} M. The Au content was measured using muffle furnace; it was found that there was 0.02 g of Au existing in 1 g of drying (CTS−Au)@CMSD nanospheres powder. To measure MEF, a certain amount of PFV solution was added to the CTS−CMSD and (CTS−Au)@CMSD nanosphere solutions (the concentration of PFV was 2×10^{-6} M) and then stirred for at least 30 min to prepare PFV-adsorbed hybrid nanospheres.

Enzymatic Degradation of (CTS−Au)@CMSD Nanospheres. (CTS−Au)@CMSD nanospheres were transferred into a mixture of pancreatin and amyloglucosidase (1000 units/mL, pH = 5−6) and incubated at 37 °C for 24 h. After degradation, the suspension was fractionated, centrifuged, and then carefully washed with deionized water at least three times. The degradation process was investigated by analyzing the evolution of the morphology of (CTS−Au)@CMSD nanospheres using ESEM.

Cytotoxicity Assay Using the MTT Method. HeLa cervical carcinoma cells were seeded into 96-well plates at a concentration of 8×10^4 cells mL^{-1} and maintained for 24 h in 1 mL of Dulbecco's Modified Eagle medium (DMEM). Different amounts of (CTS−Au)@CMSD/PFV nanosphere solution (2.0, 4.0, 6.0, 8.0, and 10.0 μL) were then added to the medium, and the cells were incubated for a further 24 h at 37 °C. After decanting off the medium, freshly prepared MTT solution (1 mg mL^{-1} in PBS, 100 μL) was added to each well and incubated for 4 h. After removing the MTT solution, the cells were lysed by adding DMSO (dimethylsulfoxide, 100 μL). The plate was gently shaken for 5 min, and then, the absorbance of purple formazan at 490 nm was monitored using a Spectra MAX 340PC plate reader. To determine the toxicity of nanospheres to cells, the same amount of CTS−CMSD nanocomposite or (CTS−Au)@CMSD nanospheres was also incubated with the cells in the MTT experiment instead of (CTS−Au)@CMSD/PFV nanospheres.

Cellular Imaging Experiments. Concentrated (CTS−Au)@CMSD/PFV nanosphere solution (50 μL) was added to DMEM medium (1 mL) containing HeLa cervical carcinoma cells in a 35 mm^2 plate ([PFV] = 1.6×10^{-6} M). The plate was then incubated for 10 h at 37 °C. Fluorescence and phase contrast bright-field image of HeLa cells were recorded on a fluorescence microscope (Olympus IX71) using a 455/70 nm excitation filter with an exposure time of 500 ms.

RESULTS AND DISCUSSION

Synthesis and Characterization of (CTS−Au)@CMSD and (CTS−Au)@CMSD/PFV Nanospheres. Au nanoparticles were synthesized using an in situ method by adding $HAuCl_4$ solution dropwise into CTS solution (pH = 5−6) and heating the mixture at 85 °C for 2.5 h.[39,40] The Au nanoparticles acted as a cross-linker in the CTS matrix during the reduction process. A CMSD shell was formed on the CTS−Au core surface through electrostatic attraction between the amino groups of CTS and carboxyl groups of CMSD. As shown in Scheme 1, using EDCI as a catalyst induced the amino groups of CTS to react with the free carboxyl groups and aldehyde groups of CMSD, forming amide bonds and Schiff base structures, respectively.[27,41,42]

The preparation process of (CTS−Au)@CMSD nanospheres is illustrated in Scheme 2. The Au nanoparticles were encapsulated by the CTS molecules, forming a CTS−Au nanocomposite with positively charged surfaces. When the nanocomposite was slowly added dropwise to a CMSD solution, the anionic CMSD adsorbed onto its surface by electrostatic interaction. Unattached CMSD molecules were removed by centrifugation to give (CTS−Au)@CMSD nanospheres. Furthermore, the number of Au nanoparticles in the CTS−Au core can be controlled by varying the concentration of aqueous $HAuCl_4$ solution. Increasing the concentration of Au ions increases the density of Au nanoparticles in the core of the (CTS−Au)@CMSD nanospheres. That is because the

Scheme 1. (a) Synthesis and Structure of CMSD. (b) Amide Bond Structure and Schiff Base Crosslinking of the (CTS−Au)@CMSD Nanospheres

redundant Au ions could still be reduced by the remaining amino groups of CTS.

To confirm the formation of covalent bonds between CTS and CMSD, FTIR spectra of CMS, CMSD, CTS, and CTS−CMSD composites were measured. Compared with that of CMS (Figure S1a, Supporting Information), the FTIR spectrum of CMSD contained a band at 1740 cm^{-1} that was consistent with the symmetric vibrations of aldehyde, indicating the formation of aldehyde groups. It should be noted that this band is weak and, in some cases, could not be detected because it was obscured by a signal from hemiacetals formed between free aldehyde groups.[43] In the spectrum of the CTS−CMSD composite, the intensity of the C═N stretching vibration at 1416 cm^{-1} increased substantially after cross-linking between CTS and CMSD, and the peaks at 1425 and 1383 cm^{-1} in the spectrum of CTS merged, indicating the formation of Schiff bases (characteristic of C═N).[44] The characteristic absorption band of the $-NH_2$ stretching vibration at 1640 cm^{-1}, which is weak in Schiff bases, is probably masked by those of the amide group at 1668 and 1600 cm^{-1}.[27] The characteristic peaks at 1156 and 1028 cm^{-1} ($\nu_{c\text{-}o\text{-}c}$ vibration of glucose ether) from both CTS and CMSD were still observed after cross-linking.[45] All of the observed changes were consistent with the formation of Schiff bases and amide bonds between CTS and CMSD after cross-linking.

To further investigate the cross-link of (CTS−Au)@CMSD hybrid nanospheres systems, additional NMR analyses were carried out. First, CMSD and CTS alone were characterized (Figure S2a and Figure S2b in Supporting Information). As shown in Figure S2a (Supporting Information), signals appeared at 9.3 ppm (Figure S2a, Supporting Information), these resonance peaks were assigned to hemiacetals. After the Schiff base reaction of aldehyde groups with $-NH_2$ group, the peak of aldehyde groups at 9.3 ppm disappeared. At the same time, a new peak assigned to the proton of −CH near the Schiff bases appeared at 2.2 ppm (Figure S2c, Supporting Information). As shown in Figure S2c (Supporting Information), another new peak appeared at 8.4 ppm. This peak may be assigned to the proton of acylamide group, which demonstrated the cross-link of the of carboxy group of CMSD with amino group of CTS. All of the results were in accordance with the mechanism as shown in Scheme 1b.

After the reduction of Au nanoparticles and covalent cross-linking of CTS and CMSD, the (CTS−Au)@CMSD nanospheres were obtained. Figure 1 shows the TEM images of the

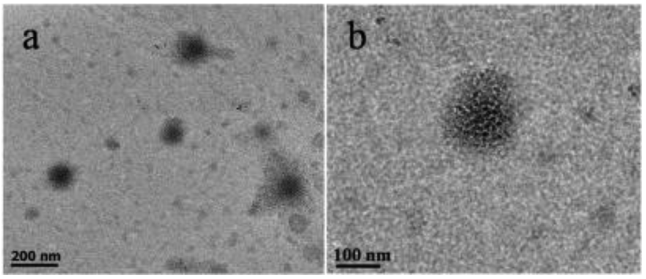

Figure 1. TEM images of (CTS−Au)@CMSD nanospheres.

(CTS−Au)@CMSD hybrid nanospheres. The hybrid nanospheres preserved their structural integrity; the brink gray region and the center dark region represented the shell and core of the nanosphere (Figure 1b). To verify that electrostatic assemblies formed between CTS and CMSD, the zeta potentials of these particles were measured. The results showed that the CTS−Au nanocomposites had a positively charged surface with a zeta potential of 43.5 mV. After adding aqueous CMSD solution, the zeta potential of the nanocomposites decreased to −21.6 mV, indicating that CMSD was successfully

Scheme 2. Schematic Illustration of the Preparation of (CTS−Au)@CMSD/PFV Nanospheres and the Chemical Structure of PFV

dx.doi.org/10.1021/am301945k | ACS Appl. Mater. Interfaces 2012, 4, 6332−6337

adsorbed onto the CTS−Au nanocomposite surfaces, producing negatively charged surfaces.

The water-soluble conjugated polymer PFV was selected as a model dye to study the MEF of the (CTS−Au)@CMSD nanospheres. Compared with small fluorescent molecules, this positively charged macromolecular dye is easy to control and assemble. Moreover, the low fluorescence quantum yield of PFV (4.5%) makes it a good candidate for MEF. Because of the negative surface of the (CTS−Au)@CMSD nanospheres, PFV could be adsorbed onto their surface by electrostatic attraction, as shown in Scheme 2. Aqueous PFV solution was mixed with a (CTS−Au)@CMSD nanosphere dispersion and then incubated for 30 min at room temperature to achieve sufficient adsorption. The zeta potential of (CTS−Au)@CMSD/PFV nanospheres was −16.9 mV, which is higher than that of −21.6 mV of the nanospheres lacking PFV. The change in zeta potential indicated that PFV molecules were successfully adsorbed onto the surface of the (CTS−Au)@CMSD nanospheres. After the (CTS−Au)@CMSD/PFV hybrid nanospheres were prepared, their MEF was measured and then they were used in cellular imaging.

MEF of (CTS−Au)@CMSD/PFV Nanospheres. To study the MEF of the (CTS−Au)@CMSD nanospheres, they were coated with PFV (the concentrations of nanospheres and PFV were 8.0×10^{-8} and 2.0×10^{-6} M, respectively). The emission spectrum was recorded 30 min after mixing to ensure that the PFV molecules were well adsorbed onto the surface of the nanospheres. The solution was excited at 437 nm, which is the maximum absorption wavelength of PFV in water. Spectra of different concentrations of (CTS−CMSD)/PFV hybrid nanospheres without Au nanoparticles and PFV solution were also measured as control experiments. As shown in Figure 2, the fluorescence intensity of PFV was further enhanced when the Au nanoparticles were introduced into the system, with an enhancement factor of about 1.43 compared with that of (CTS−CMSD)/PFV nanospheres and of about 2.00 compared with PFV solution. According to previous work in our group,[15] the increased fluorescence intensity of PFV may be attributed to two effects. Au nanoparticles present in the core of the nanospheres, whose surface plasmon resonance may increase the excitation efficiency or decrease the nonradiative decay of the dye. In this system, we also find that (CTS−CMSD)/PFV hybrid nanospheres without Au nanoparticles can increase the enhancement factor of about 1.3 compared with pure PFV solution. It is perhaps due to the reason that the polymers could reduce the self-aggregation and self-quenching of PFV molecules by providing a more hydrophobic environment than water.[46]

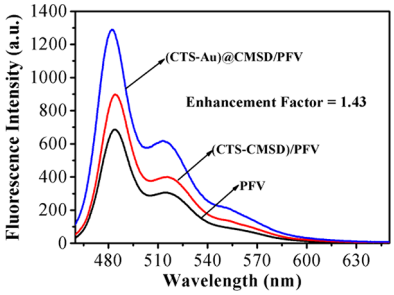

Figure 2. Fluorescence spectra of PFV, (CTS−CMSD)/PFV nanospheres, and (CTS−Au)@CMSD/PFV hybrid nanospheres. The concentration of PFV is 2×10^{-6} mol/L.

It is known that the distance between metal and dye is a very important factor in MEF. If the dye is too close to the metal, its fluorescence is quenched, and there is no interaction if the distance is too large. Therefore, MEF is only detected within a certain range. In this system, the Au nanoparticles synthesized by in situ method in CTS were dispersed randomly in nanospheres. Thus, the observation of fluorescence enhancement indicated that the average distance between the Au nanoparticles and dye was suitable for MEF.

Degradability of (CTS−Au)@CMSD Nanospheres. Because CTS and CMSD are degradable, the (CTS−Au)@CMSD nanospheres should also exhibit good degradability. The degradability of the hybrid nanospheres was investigated using pancreatin and amyloglucosidase as the enzymes for the degradation experiments.[47,48] In the experiments, the (CTS−Au)@CMSD nanospheres were exposed to a mixture of pancreatin and amyloglucosidase (3.3 μM, pH = 5−6) at 37 °C for 24 h. ESEM images were recorded before and after enzyme addition to study the degradation behavior of the hybrid nanospheres (Figure 3). Before the enzymatic reaction, the (CTS−Au)@CMSD nanospheres were spherical structures, as shown in Figure 3a,b. After degradation for several hours, the spherical morphology changed to concave shapes including folds. The CTS/CMSD layer desorbed from the surface of the nanospheres by enzymatic degradation, possibly through the formation of water-soluble oligosaccharide units. The shell of the nanospheres became thinner and weaker as enzymatic degradation progressed, eventually leading to the destruction of the core−shell nanospheres. After 24 h, almost all of the nanospheres had degraded (Figure 3c). This finding demonstrates that the (CTS−Au)@CMSD nanospheres possess excellent biodegradability, making them suitable for biological applications.

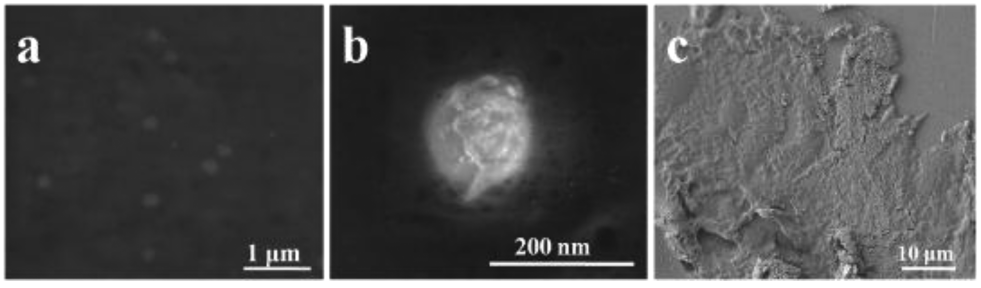

Figure 3. ESEM images of (CTS−Au)@CMSD nanospheres (a, b) before and (c) after exposure to a mixture of pancreatin and amyloglucosidase (3 μM) at 37 °C for 12 h.

(CTS−Au)@CMSD/PFV Nanospheres for Cellular Imaging. PFV has good cytocompatibility, and it has been used in biological imaging and electroactive biomaterials in human tissue engineering.[15] Au nanoparticles exhibit good biocompatibility and are well suited for in vivo applications with humans,[18] so we used the (CTS−Au)@CMSD/PFV nanospheres to visualize HeLa cervical carcinoma cells to determine the suitability of the new hybrid nanospheres in bioimaging applications. First, the cytotoxicity of the (CTS−Au)@CMSD/PFV nanospheres was investigated using the MTT cell viability assay; both (CTS−Au)@CMSD nanospheres and the CTS−CMSD nanocomposite were used as controls. The absorbance of MTT at 490 nm is dependent on the degree of metabolic viability of the cells. Thus, cell viability can be expressed by the ratio of the absorbance of the cells incubated with nanospheres or nanocomposite to that of the cells incubated with culture medium only. As shown in Figure 4, the cell viability was close

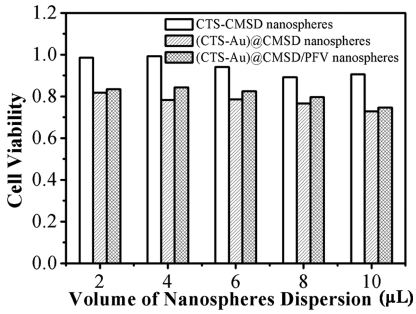

Figure 4. Cell viability results after incubation of HeLa cells with various amounts of nanospheres (2−10 μL). The cell viability calculated relative to that of the cells without adding nanospheres is defined as a viability of 1.

to 1 after incubation of HeLa cells for 24 h when 2.0 μL of CTS−CMSD nanosphere solution was added and remained higher than 0.9 when 10.0 μL of CTS−CMSD nanosphere solution was incubated with the cells. For the (CTS−Au)@CMSD/PFV nanosphere solutions, the cell viability was 84 and 74% when 2.0 and 10.0 μL of the (CTS−Au)@CMSD/PFV nanospheres was added, respectively. The concentration of PFV in the mixture was 8×10^{-7} M when 10 μL of (CTS−Au)@CMSD/PFV nanosphere solution was added. The cytotoxicity of the (CTS−Au)@CMSD nanospheres was very similar to that of the (CTS−Au)@CMSD/PFV nanospheres as the amount of nanospheres added was changed. Such concentration-dependent toxicity is proposed to be mainly caused by incubation with nanospheres in high dosages, which may retard cell proliferation and damage cell membranes. Overall, these experiments indicated that the (CTS−Au)@CMSD/PFV nanospheres had very low cytotoxicity.

Cellular imaging was conducted using the (CTS−Au)@CMSD/PFV nanospheres. Concentrated nanosphere solution was added to 1 mL of the culture medium of HeLa cervical carcinoma cells (the final concentration of PFV was 1.6 μM). Fluorescence images of HeLa were recorded after coculturing with (CTS−Au)@CMSD/PFV for 10 h at 37 °C and washing three times with PBS buffer (pH = 7.4). Figure 5b,c shows bright-field and fluorescence images of the HeLa cells cocultured with (CTS−Au)@CMSD/PFV nanospheres, respectively. The fluorescence image shows that the HeLa cells were well stained with the (CTS−Au)@CMSD/PFV nanospheres, indicating that the (CTS−Au)@CMSD/PFV nanospheres were readily internalized by the HeLa cervical carcinoma cells. This observation implies that the (CTS−Au)@CMSD/PFV nanospheres are suitable for fluorescent labeling and sensing in cellular environments.

CONCLUSION

In conclusion, novel (CTS−Au)@CMSD core−shell hybrid nanospheres were prepared by self-assembly. FTIR spectra and NMR data demonstrated the formation of covalent bonds between CTS and CMSD, increasing the stability of the core−shell structure. PFV was adsorbed onto the surface of the (CTS−Au)@CMSD nanospheres to form fluorescent hybrid nanospheres that displayed MEF. The (CTS−Au)@CMSD/PFV nanospheres exhibited good biodegradability and were readily degraded by pancreatin and amyloglucosidase. In addition, the hybrid nanospheres showed low cytotoxicity in an MTT cell viability assay and displayed bright fluorescence in a cell−imaging experiment when they were cocultured with HeLa cells. The results demonstrate that the (CTS−Au)@CMSD nanospheres possess good biocompatible properties, making them suitable for applications such as cellular labeling and sensing in vitro. Further optimization of hybrid nanospheres and modification of the fluorophore may produce nanospheres with bright fluorescence, high cytocompatibility, and tunable morphology and size that are suitable for targeted biological imaging applications.

ASSOCIATED CONTENT

Supporting Information

FTIR spectra and ^{1}H NMR spectra of CMS, CMSD, CTS, and CTS−CMSD. This material is available free of charge via the Internet at http://pubs.acs.org.

AUTHOR INFORMATION

Corresponding Author

*E-mail: lidong@mater.ustb.edu.cn.

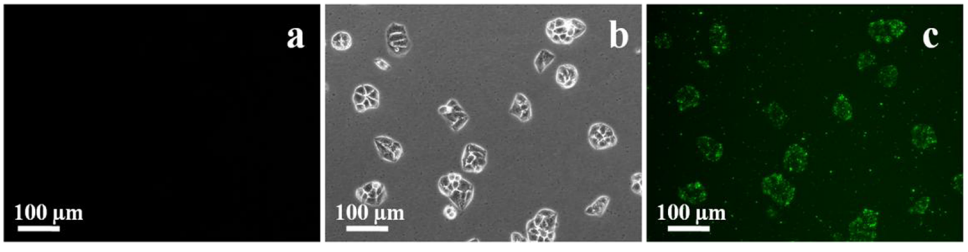

Figure 5. (a) Fluorescence image of HeLa cells without treatment of nanospheres. (b) Bright-field and (c) fluorescence images of HeLa cells cocultured with (CTS−Au)@CMSD/PFV nanospheres for 10 h at 37 °C.

Notes

The authors declare no competing financial interest.

■ ACKNOWLEDGMENTS

This research was financially supported by the National Natural Science Foundation of China (20904003, 90923015), the General Financial Grant from the China Postdoctoral Science Foundation (2011M500235), the Fundamental Research Funds for the Central Universities of China (FRT-TP-09-006A, FRT-TP-09-011B), the State Key Lab for Advanced Metals and Materials (2012-ZD05), and the Program for New Century Excellent Talents in University of Ministry of Education of China (NCET-11-0576). We are grateful to Dr. Libing Liu and Ms. Huanxiang Yuan (Institute of Chemistry, CAS, Beijing) for their kind support for the cellular experiments.

■ REFERENCES

(1) Chaudhuri, R. G.; Paria, S. *Chem. Rev.* **2012**, *112*, 2373−2433.
(2) Zheng, D.; Seferos, D. S.; Giljohann, D. A.; Patel, P. C.; Mirkin, C. A. *Nano Lett.* **2009**, *9*, 3258−3261.
(3) Nam, J.-M.; Stoeva, S. I.; Mirkin, C. A. *J. Am. Chem. Soc.* **2004**, *126*, 5932−5933.
(4) Lee, W.; Kim, M. G.; Choi, J.; Park, J.; Ko, S. J.; Oh, S. J.; Cheon, J. *J. Am. Chem. Soc.* **2005**, *127*, 16090−16097.
(5) Law, W.-C.; Yong, K.-T.; Roy, I.; Ding, H.; Hu, R.; Zhao, W.; Prasad, P. N. *Small* **2005**, *5*, 1302−1310.
(6) Katti, K. S. *Colloids Surf., B* **2004**, *39*, 133−142.
(7) Ow, H.; Larson, D. R.; Srivastava, M.; Baird, B. A.; Webb, W. W.; Wiesner, U. *Nano Lett.* **2005**, *5*, 113−117.
(8) Jin, Y.; Li, A.; Hazelton, S. G.; Liang, S.; John, C. L.; Selid, P. D.; Pierce, D. T.; Zhao, J. X. *Coord. Chem. Rev.* **2009**, *253*, 2998−3014.
(9) Louis, C.; Bazzi, R.; Marquette, C. A.; Bridot, J.-L.; Roux, S.; Ledoux, G.; Mercier, B.; Blum, L.; Perriat, P.; Tillement, O. *Chem. Mater.* **2005**, *17*, 1673−1682.
(10) Zhang, R.; Wu, C.; Tong, L.; Tang, B.; Xu, Q.-H. *Langmuir* **2009**, *25*, 10153−10158.
(11) Zhang, Y.; Wang, L.; Tian, J.; Li, H.; Luo, Y.; Sun, X. *Langmuir* **2011**, *27*, 2170−2175.
(12) Tang, F.; Ma, N.; Wang, X.; He, F.; Li, L. *J. Mater. Chem.* **2011**, *21*, 16943−16948.
(13) Cheng, D.; Xu, Q. H. *Chem. Commun.* **2007**, 248−250.
(14) Liu, J.; Li, A.; Tang, J.; Wang, R.; Kong, N.; Davis, T. P. *Chem. Commun.* **2012**, *48*, 4680−4682.
(15) Tang, F.; He, F.; Cheng, H.; Li, L. *Langmuir* **2010**, *26*, 11774−11778.
(16) Yang, J.; Zhang, F.; Chen, Y.; Qian, S.; Hu, P.; Li, W.; Deng, Y.; Fang, Y.; Han, L.; Luqman, M.; Zhao, D. *Chem. Commun.* **2011**, *47*, 11618−11620.
(17) Lawal, O. S.; Storz, J.; Storz, H.; Lohmann, D.; Lechner, D.; Kulicke, W.-M. *Eur. Polym. J.* **2009**, *45*, 3399−3408.
(18) Huang, H.; Yang, X. *Colloids Surf., A: Physicochem. Eng. Aspects* **2003**, *226*, 77−86.
(19) Wang, B.; Chen, K.; Jiang, S.; Reincke, F.; Tong, W.; Wang, D.; Gao, C. *Biomacromolecules* **2006**, *7*, 1203−1209.
(20) Ding, L.; Hao, C.; Xue, Y.; Ju, H. *Biomacromolecules* **2007**, *8*, 1341−1346.
(21) Wei, D.; Ye, Y.; Jia, X.; Yuan, C.; Qian, W. *Carbohydr. Res.* **2010**, *345*, 74−81.
(22) Hortigüela, M. J.; Aranaz, I.; Gutiérrez, M. C.; Ferrer, M. L.; del Monte, F. *Biomacromolecules* **2011**, *12*, 179−186.
(23) Saboktakina, M. R.; Tabatabaie, R. M.; Maharramov, A.; Ramazanov, M. A. *Int. J. Biol. Macromol.* **2011**, *48*, 381−385.
(24) Sloan, J. W.; Mehltretter, C. L.; Senti, F. R. *J. Chem. Eng. Data* **1962**, *7*, 156−158.
(25) Hattori, M.; Yang, W.; Takahashi, K. *J. Agric. Food Chem.* **1995**, *43*, 2007−2011.
(26) Wang, Y. J.; Assaad, E.; Ispas-Szabo, P.; Mateescu, M. A.; Zhu, X. X. *Int. J. Pharm.* **2011**, *419*, 215−221.
(27) Assaad, E.; Wang, Y. J.; Zhu, X. X.; Mateescu, M. A. *Carbohydr. Polym.* **2011**, *84*, 1399−1407.
(28) Jones, M. R.; Osberg, K. D.; Macfarlane, R. J.; Langille, M. R.; Mirkin, C. A. *Chem. Rev.* **2011**, *111*, 3736−3827.
(29) Geddes, C. D.; Lakowicz, J. R. *J. Fluoresc.* **2002**, *2*, 121−129.
(30) Szmacinski, H.; Badugu, R.; Lakowicz, J. R. *J. Phys. Chem. C* **2010**, *114*, 21142−21149.
(31) Fu, Y.; Lakowicz, J. R. *J. Phys. Chem. C* **2010**, *114*, 7492−7495.
(32) Zhang, J.; Lakowicz, J. R. *J. Phys. Chem. B* **2006**, *110*, 2387−2392.
(33) Ma, N.; Tang, F.; Wang, X.; He, F.; Li, L. *Macromol. Rapid Commun.* **2011**, *32*, 587−592.
(34) Tong, L.; Ma, N.; Tang, F.; Qiu, D.; Cui, Q.; Li, L. *J. Mater. Chem.* **2012**, *22*, 8988−8993.
(35) Zhang, J.; Ma, N.; Tang, F.; Cui, Q.; He, F.; Li, L. *ACS Appl. Mater. Interfaces* **2012**, *4*, 1747−1751.
(36) Doane, T. L.; Burda, C. *Chem. Soc. Rev.* **2012**, *41*, 2885−2911.
(37) Dhar, N.; Akhlaghi, S. P.; Tam, K. C. *Carbohydr. Polym.* **2012**, *87*, 101−109.
(38) Zhang, S.; Wang, X.; Zhang, Y.; Yang, K.; Wang, Y. *J. Polym. Res.* **2010**, *17*, 439−446.
(39) Ahn, S.; Jung, S. Y.; Kim, B. H.; Lee, S. J. *Acta Biomater.* **2011**, *7*, 2139−2147.
(40) Miyama, T.; Yonezawa, Y. *Langmuir* **2004**, *20*, 5918−5923.
(41) Saboktakin, M. R.; Tabatabaie, R. M.; Maharramov, A.; Ramazanov, M. A. *Int. J. Biol. Macromol.* **2011**, *48*, 381−385.
(42) Xia, B.; Cui, Q.; He, F.; Li, L. *Langmuir* **2012**, *28*, 11188−11194.
(43) DiFlavio, J.-L.; Pelton, R.; Leduc, M.; Champ, S.; Essig, M.; Frechen, T. *Cellulose* **2007**, *14*, 257−268.
(44) Wang, J.; Fu, W.; Zhang, D.; Yu, X.; Li, J.; Wan, C. *Carbohydr. Polym.* **2010**, *79*, 705−710.
(45) Zhao, Q. H.; Mao, Z. W.; Gao, C. Y.; Shen, J. C. *J. Biomater. Sci., Polym. Ed.* **2006**, *17*, 997−1014.
(46) Jiang, X.; Lavender, C. A.; Woodcock, J. W.; Zhao, B. *Macromolecules* **2008**, *41*, 2632−2643.
(47) Jia, Y.; Fei, J.; Cui, Y.; Yang, Y.; Gao, L.; Li, J. *Chem. Commun.* **2011**, *47*, 1175−1177.
(48) Itoh, Y. K.; Matsusaki, M.; Kida, T.; Akashi, M. *Biomacromolecules* **2006**, *7*, 2715−2718.